

# The High Resolution Diffraction Beamline P08 at PETRA III

Oliver. H Seeck, Carsten Deiter      Hasylab @ DESY, Hamburg  
08.Sep. 2009

## Introduction

Frequently, the use of highly brilliant synchrotron x-ray radiation is mandatory if properties of bulk, surfaces and interfaces are investigated. For this, at the research center DESY in Hamburg (Germany) the new third generation synchrotron radiation source PETRA III has been built. PETRA III is especially designed to generate x-ray beams with very small divergence and source size, high intensity and very good coherence properties. Nine sectors for x-ray and VUV experiments are available. They are equipped with either one long undulator (5m or longer) or two 2m undulators. In the latter case both 2m undulators will be oriented not exactly in-line but slightly horizontally canted by 5mrad. This canting angle is sufficiently large to install two completely independent beamlines in one sector. This is the case at Sector 6 with the two beamlines P08 and P09 for x-ray scattering and diffraction applications. Beamline P08 is designed for experiments which require very high resolving power in reciprocal space and/or in real space.

P08 is perfectly suited for investigations of bulk samples, surfaces and interfaces. The x-ray beam parameters at the sample can be chosen in a wide range: Photon energies can be set between 5keV and 30keV and scanned in a 100eV interval. The beam size can be shaped to values between 2mm×1mm and 5µm×1µm (in the µ-focusing mode, all figures horizontal×vertical). The beam divergence can be as low as 8µrad×0.5µrad (in collimation mode). The photon energy band width is usually about  $10^{-5}$  with a total flux at the sample of  $10^{12}$  ph/sec.

In the experimental area a high precision 6-circle diffractometer and a liquid diffractometer are installed. Many different methods to investigate bulk, surfaces and interfaces of solids and liquids are available. Diffraction based methods are single crystal and powder diffraction, Crystal Truncation Rod (CTR) measurements, Grazing Incidence Diffraction (GID) and X-ray Standing Wave (XWS) measurements. Scattering based methods are reflectivity and Grazing Incidence Small Angle Scattering (GISAXS). Coherence applications such as X-ray Photon Correlation Spectroscopy (XPCS) may also be possible though P08 is not explicitly optimized for maintaining the coherence properties of the x-ray beam.

## REFERENCES

1. H.Franz, O. Leupold, R. Röhlberger, S.V. Roth, O.H. Seeck, J. Spengler, J. Stempfner, M. Tischer, J. Viefhaus, E. Weckert, and T. Wroblewski, *Synch. Rad. News* 6, 25-29 (2006)
2. K. Balewski, W. Brefeld, W. Decking, H. Franz, R. Röhlberger, E. Weckert, *PETRA III: A Low Emittance Synchrotron Radiation Source*, DESY Press, 2004.
3. O. Magnussen, J. Stettner, M. Tolan, *Röntgendiffraktometer zur Untersuchung von Flüssigkeitsgrenzflächen an PETRA III*, BMBF 05 KS7Fk3, 2007.

## The Scope of HighRes

High resolution X-ray diffraction (HRXRD) is traditionally used for precise measurements of lattice parameters and is widely used as a standard tool for structural investigations. HRXRD allows to determine physical parameters of single crystals, for instance thermal expansion coefficients and phase transition parameters. Also precise measurements of strain and stress distribution at the level of relative lattice parameter variations of  $10^{-4}$  –  $10^{-6}$  in the bulk and at interfaces are possible. Lattice distortions induced by various defects can be studied from their influence on the shape and the width of reflection profiles.

Investigations using HRXRD cover different of length scales:

- Atomic scale: The atomic structure and charge density in bulk, and layers as well as at surfaces and interfaces can be resolved with x-ray diffraction methods. It is the most accurate probe to determine the positions, occupation factors and displacement parameters of atoms within the unit cell. Even charge density studies on the level of binding electrons are feasible.
- Nanometer scale: For structures at solid and liquid surfaces and at buried interfaces HRXRD allows to define parameters such as thickness, orientation, chemical composition and interface roughness of layers. By variation of the incidence angle in reflectometry and grazing incidence diffraction/scattering also depth-resolved studies can be carried out. Two-dimensional reciprocal space mapping methods can be used to investigate anisotropic samples surfaces.
- Micrometer scale: Structural parameters of periodic and non-periodic nano structures and organic/inorganic material systems at mesoscopic length scales can be investigated. Also for these techniques reciprocal space mapping is standard.

High resolution can be defined in real space (such as sub-nanometer resolution) or in reciprocal space, where the real space and the reciprocal space are connected by a Fourier transformation. In contrast to many other beamlines, at P08 “high resolution” will be available in real AND in reciprocal space. This means extraordinary accurate translations and in rotations over a very large range and in all degrees of freedom. For this reason, P08 is equipped with high precision diffractometers which enable the user to position and orient the sample and the x-ray beam without any restrictions.

Additionally to HRXRD, P08 has more general scattering methods available which enables the user to investigate also amorphous or liquid samples in all varieties (see Fig 1). With some restrictions, easy spectrometric methods such as fluorescence analysis and anomalous scattering can be used as a supplement.

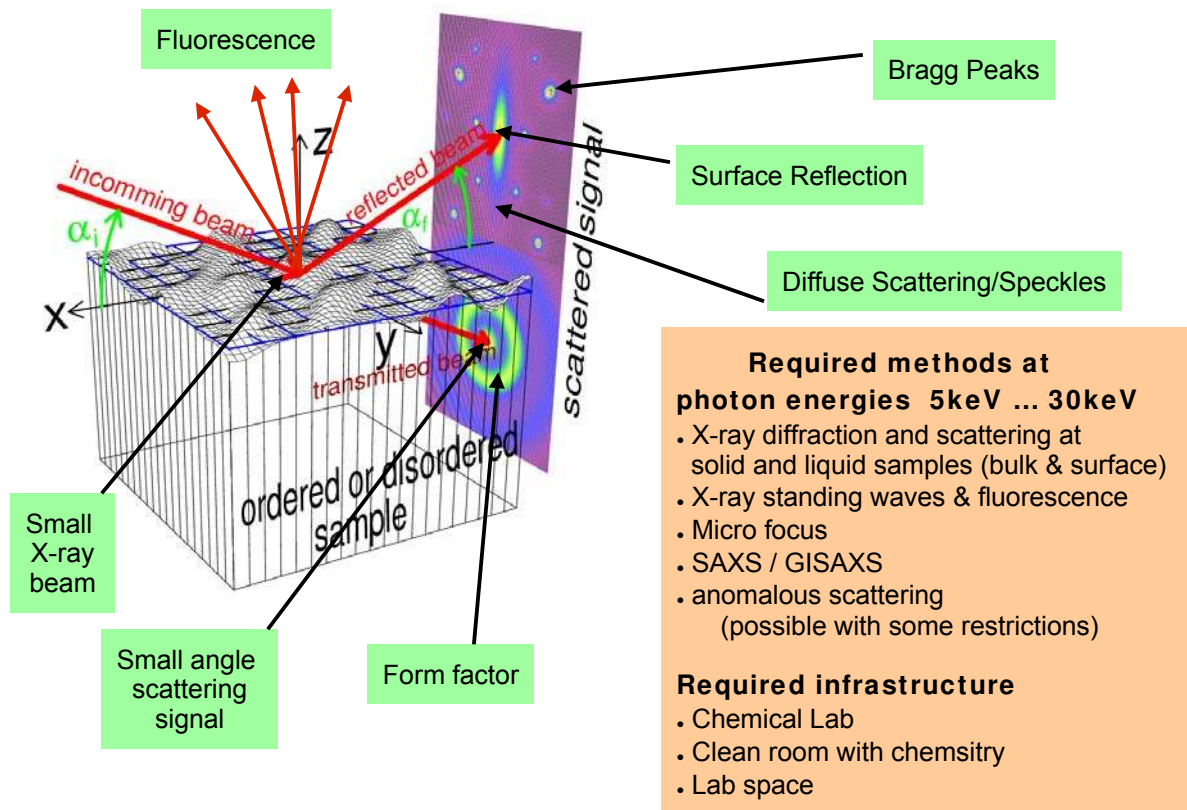


Figure 1: Methods which are available at P08

### The storage ring PETRA III

The PETRA III storage ring is a third generation synchrotron radiation source. It delivers x-ray beams from the VUV-range (50eV) to the hard energy range (200keV). In this photon energy range the beam parameters are optimized in terms of flux, small divergence, small beam size and narrow energy band with. This means to optimize the “average brilliance”  $B$  which is defined as

$$B = \frac{\text{Number of Photons}}{\text{Time} \cdot \text{horizontal Size} \cdot \text{vertical Size} \cdot \text{horizontal Divergence} \cdot \text{vertical Divergence} \cdot \text{Band Width}}$$

with the usual units  $1/(\text{s} \cdot \text{mrad}^2 \cdot \text{mm}^2 \cdot 0.1\% \text{BW})$ .

The storage ring parameters which are relevant for the x-ray beam properties are listed in Table 1.

Table 1: Overview of the relevant PETRA III ring parameters. The current will be 100mA during the first phase and 200mA in a later stage.

Circumference:	2204 m	Particle Energy:	6 GeV
Current :	100(200) mA	Horizontal Emittance:	1 nmrad
Coupling Constant:	0.01	Bunch length:	13.2 mm
No. of Bunches (continuous):	960	No. of Bunches (timing):	40
Radiation Power (Damping Wiggler):	351kW		

With this parameters and adequately designed x-ray sources, namely the undulators, PETRA III is superior over other 3rd generation sources in terms of beam quality. The photon flux is comparable to the other sources. The gain over other sources is caused by the small beam size and the small beam divergence which enter into the brilliance (see Fig. 2).

Another property which is not addressed yet is the coherence. Basically, the coherence of undulator-based x-ray radiation is determined by the source size, the wavelength and the distance source – sample. Additionally, the source size determines the ability to focus the beam. Small source size and long distances mean good coherence properties and small focal spot on the sample. The source parameters can be changed by tuning the so-called  $\beta$ -function. Table 2 lists the source parameters of a 5m long PETRA III standard undulator depending on the  $\beta$ -function.

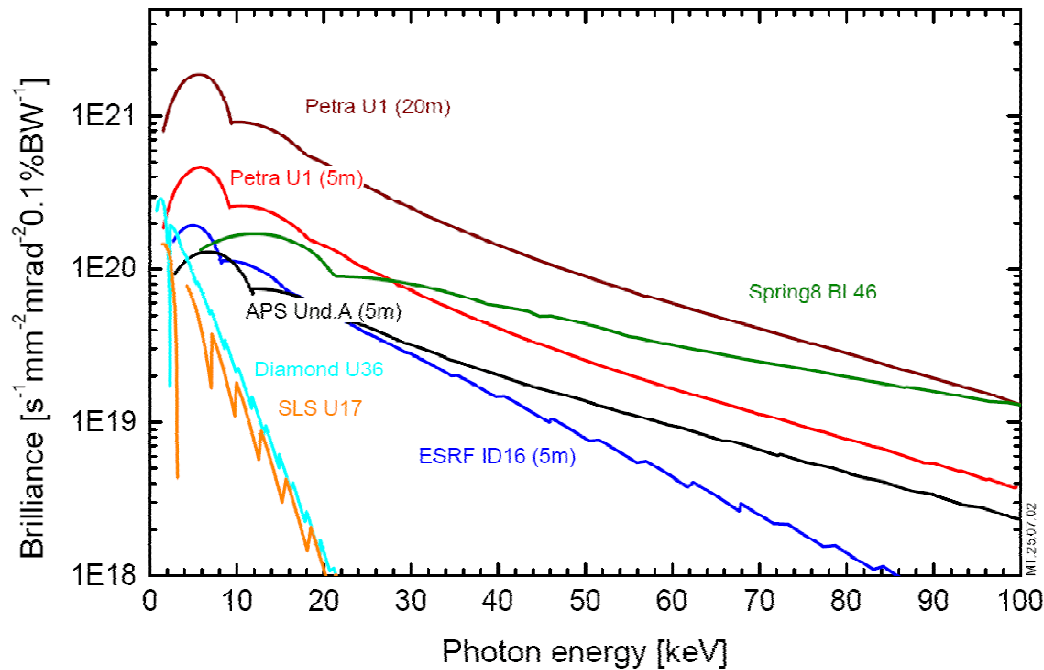


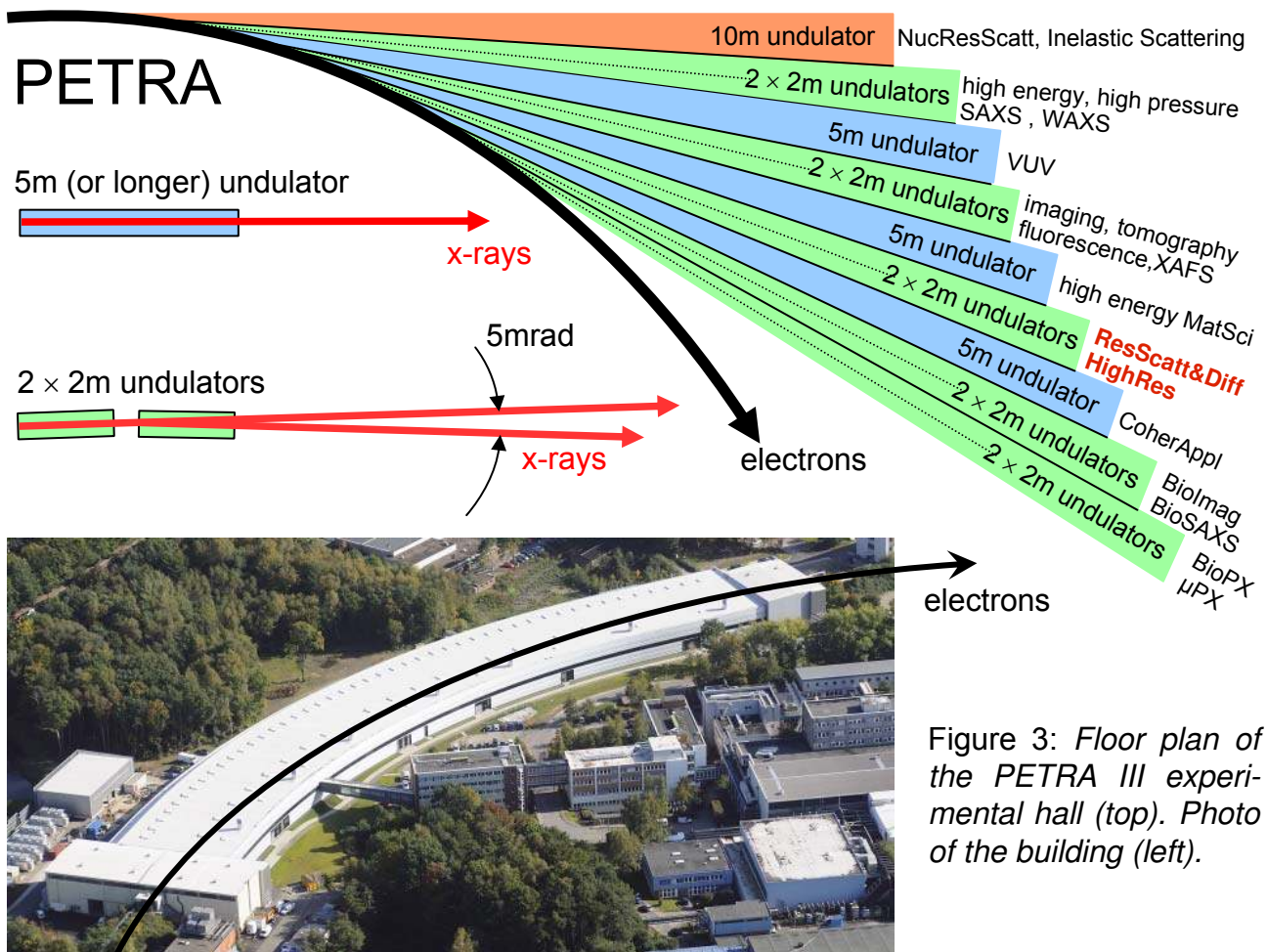
Figure 2: Brilliance plots of the modern synchrotron radiation sources

Table 1: Overview of  $\beta$  - functions, photon source sizes  $\Sigma_{x,y}$  and divergences  $\Sigma_{x',y'}$  of PETRA III at the source position. The parameters are given for a photon energy of 12 keV and 5m undulator length. All values are rms.

	$\beta_x$	$\beta_y$	$\Sigma_x$	$\Sigma_y$	$\Sigma_{x'}$	$\Sigma_{y'}$
	[m]	[m]	[ $\mu\text{m}$ ]	[ $\mu\text{m}$ ]	[ $\mu\text{rad}$ ]	[ $\mu\text{rad}$ ]
low $\beta$	1.2	4	34.5	7.3	29	5.2
high $\beta$	20	2.38	141	4.2	8.6	5.2

### The experimental hall at PETRA III (Bldg 47c)

The experimental hall is approximately 300m long and roofs one octant of the PETRA III storage ring and houses 9 sectors with 14 beamlines. Each of the beamlines is specialized on particular x-ray methods which as displayed in Fig. 3.



## The P08 beamline set-up

Beamline P08 is sub-divided into five major parts:

- 1) The frontend, containing the x-ray source (undulator), the white beam slits and safety equipment.
- 2) The optics hut, containing the monochromators which select the desired x-ray wavelength and compound refractive beryllium lenses (CRLs) to focus or collimate the beam.
- 3) The experimental hut, containing the 6-circle diffractometer, a liquid diffractometer and two optical tables with 5 degrees of freedom.
- 4) The control hut, containing the electronics, computers and a small chemical fume hood.
- 5) The laboratories. One general lab for P08 exists, a mechanical and an electrical lab is shared with the Resonant Scattering Beamline P09. A chemical lab and chemical cleanroom is available for all PETRA III users.

### The frontend

At the frontend of P08 the standard 2m undulator U29-2 with a magnetic period of 29mm, a horizontal  $\beta$ -value of 16.15m and a vertical b-value of 2.61m is installed. The minimum gap of the undulator is 9.5mm. The standard undulator is optimized for delivering high flux over the full photon energy range (see Fig. 4).

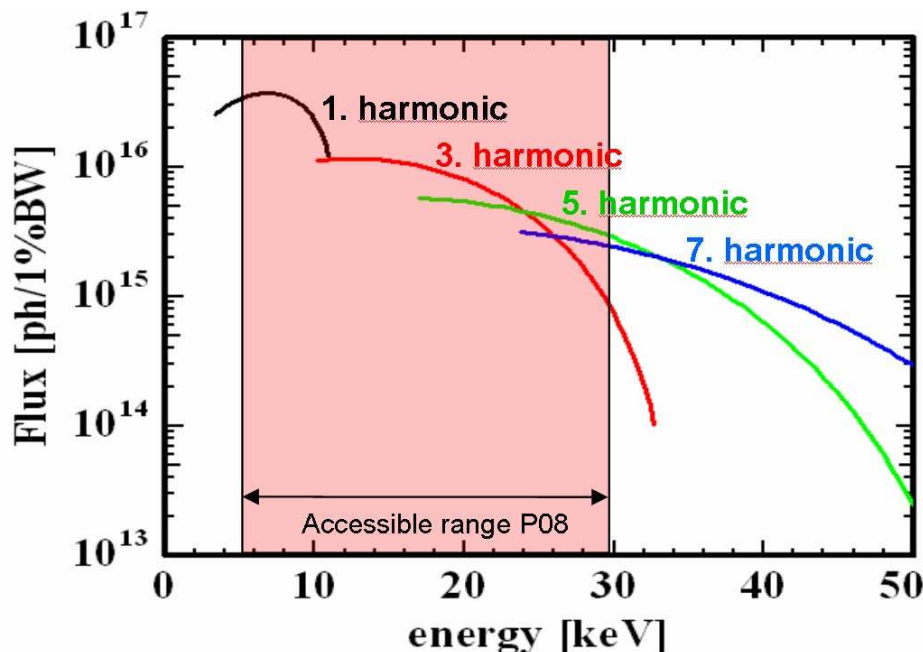


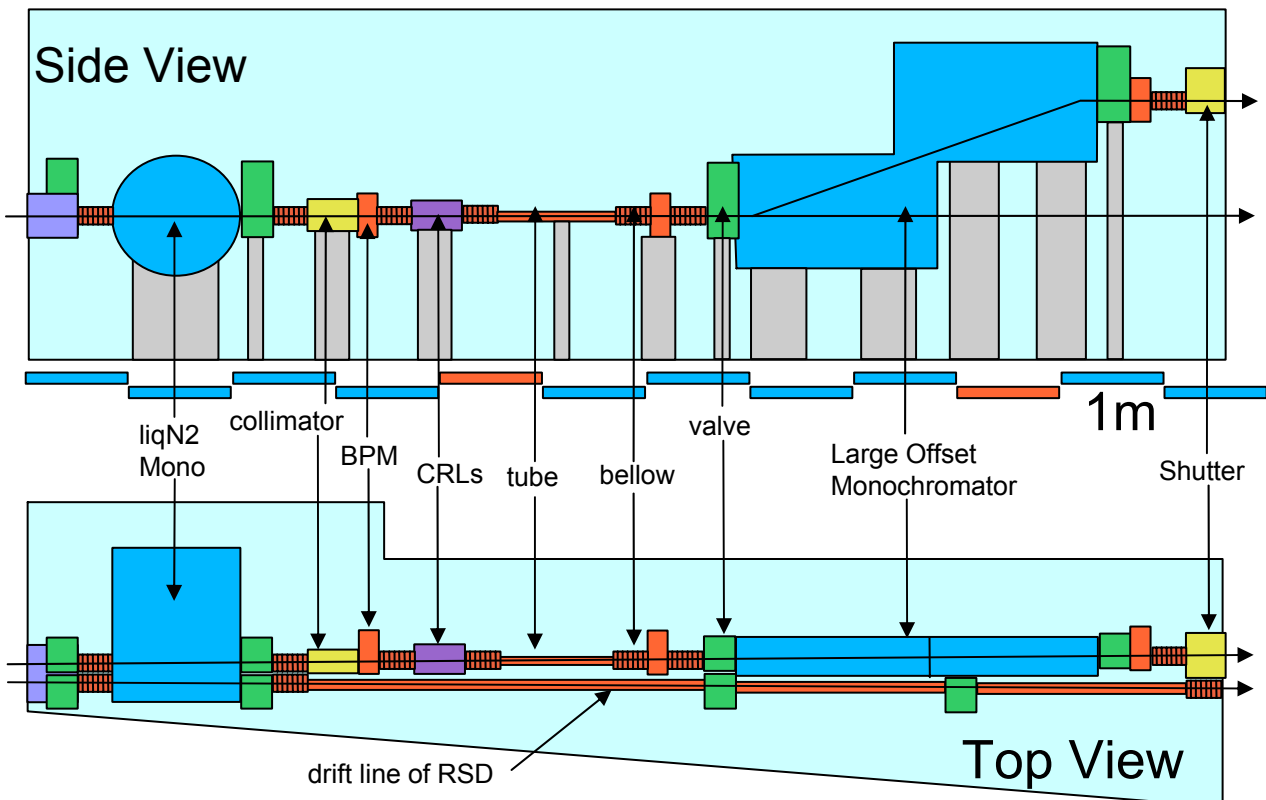
Figure 4: Total flux of the undulator of the shown undulator harmonics at beam-line P08.

Furthermore, the frontend contains high power slits to define the beam size and graphite foils which can optionally be used to suppress unwanted low energy photons.

## The optics

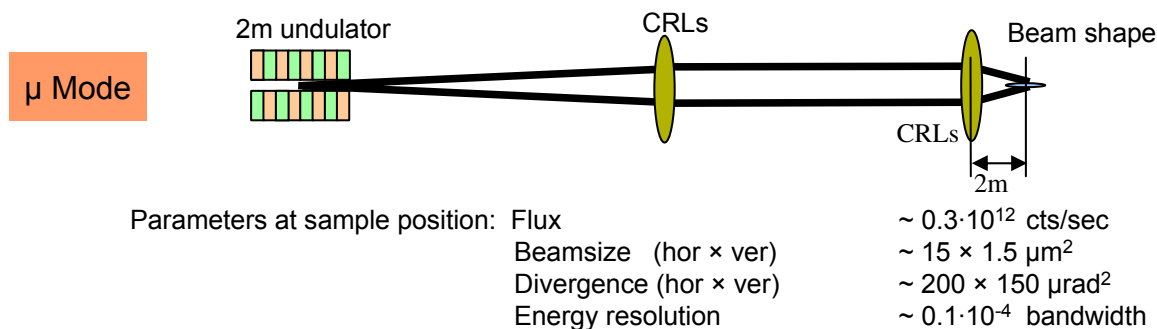
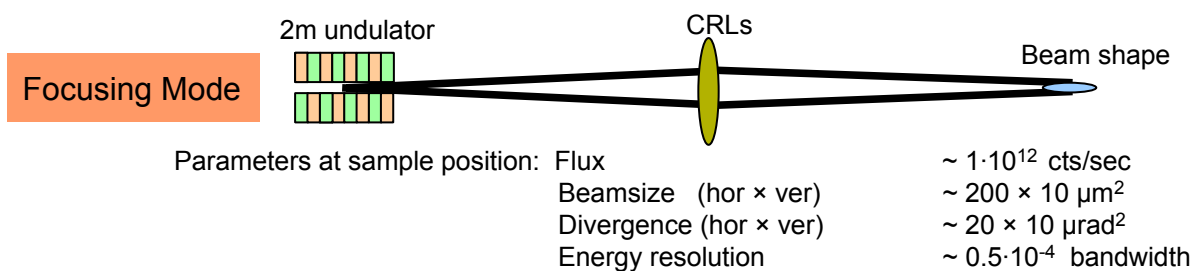
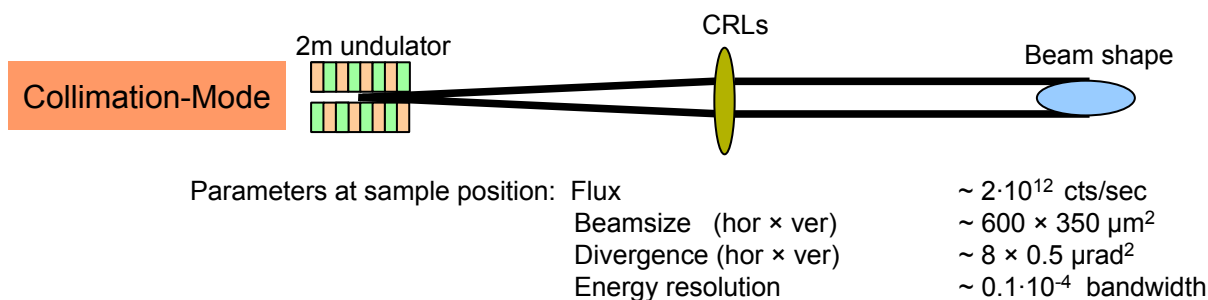
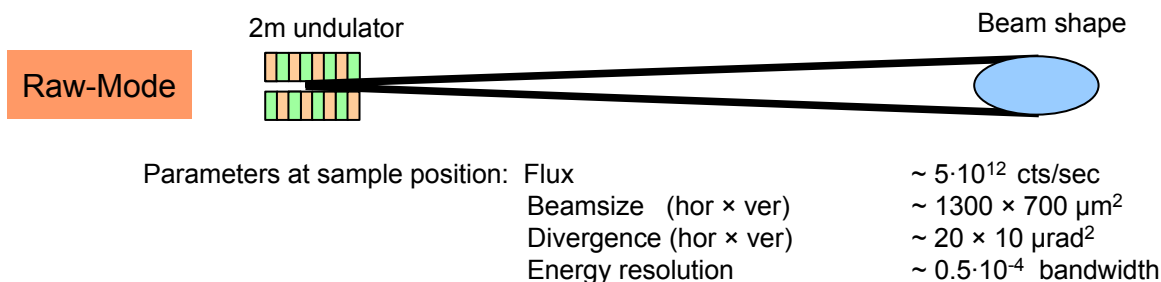
A sketch of the optics of P08 is depicted in Fig 5. The white x-ray beam is first monochromatized at the liquid nitrogen cooled monochromator. Two beam position monitors (BPMs) right after this device enable x-ray beam stabilization by means of horizontal and vertical position and direction (accuracy better  $5\mu\text{m}$  in position and better  $1\mu\text{rad}$  in direction). Optional compound refractive lenses can be used to collimate the x-ray beam (compensation of divergence) or to slightly focus the beam. The large offset monochromator (LOM) is specially designed 1) to lift the beam up by 1.25m, 2) to increase the resolving power of the x-ray beam and 3) to suppress the higher harmonic contamination of the x-rays. Not drawn is another set of two BPMs after the LOM to further stabilize the beam. Also, a second set of CRLs close to the sample position which enables micro-focusing is not shown in Fig. 5.

Figure 5: Sketch of the P08 optics. The beam comes from the left and enters the optics hutch at 33m from the undulator source. CRLs means compound refractive lenses, BPM means beam position monitor.



With this optical setup the beamline can run in four different modes. 1) the *raw-mode* for maximum flux, 2) the *collimation-mode* for highest resolving power in reciprocal space, 3) the *focusing-mode* for moderate focusing with still high resolving power and 4) the  $\mu$ -*mode* for micrometer sized focal spot of the x-rays at the sample position.

The different modes can be selected by choosing adequate combinations of CRLs in the optics hutch and/or in front of the sample position. In the following the calculated x-ray beam parameters at the sample position are displayed for each of the modes.





## 1) The raw-mode

In the raw-mode no CRLs are used. The beam profile is not altered. See Figure 6 for the calculated beam parameters. The beam size at the sample is  $1.5 \times 1 \text{ mm}^2$ , the divergence  $10 \text{ } \mu\text{rad}$  vertically.

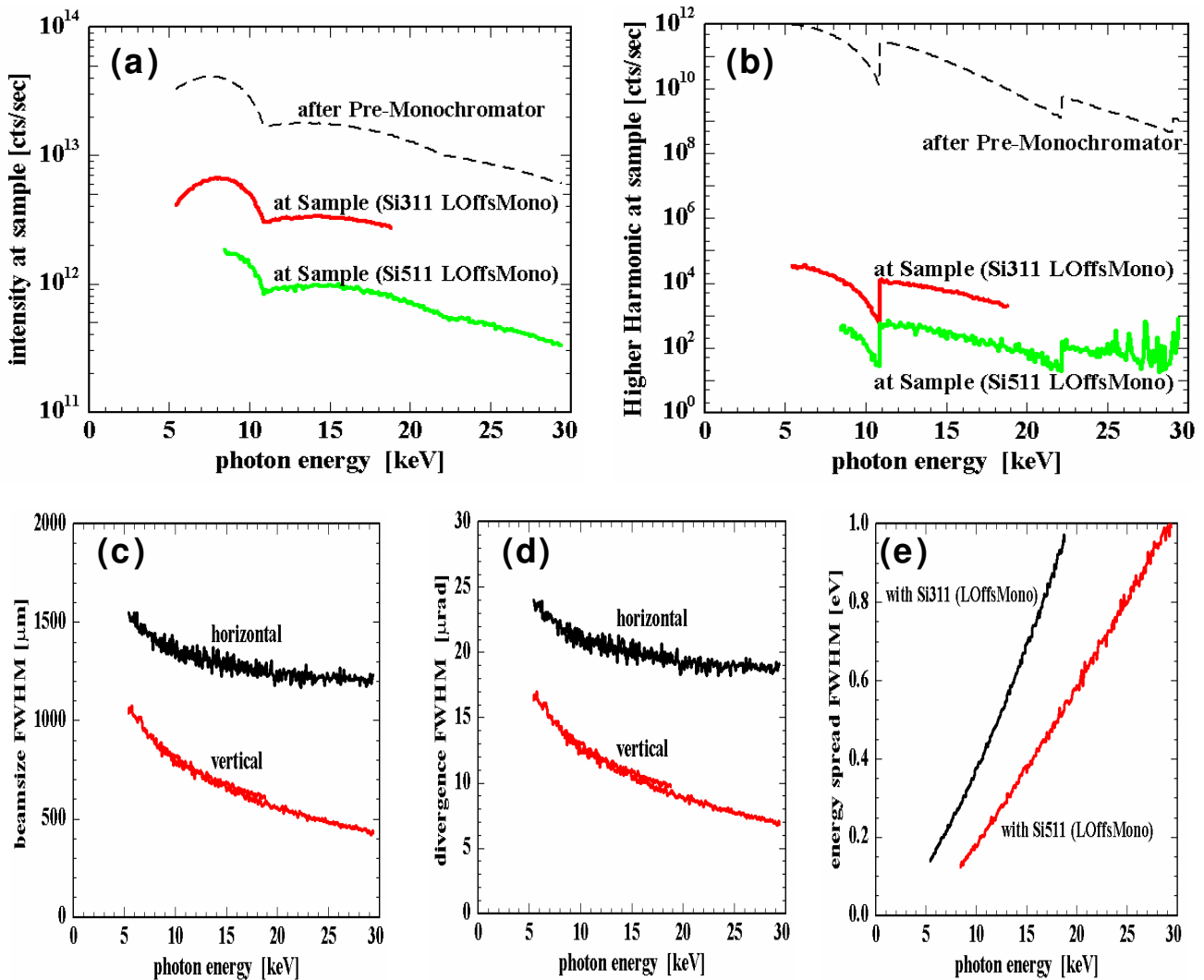


Figure 6: Parameters of the x-ray beam at the sample position using the raw-mode at P08. Displayed are: (a) the intensity in counts per second, (b) the contamination due to higher harmonic photons in counts per seconds, (c) the beam size in  $\mu\text{m}$  (FWHM), (d) the divergence in  $\mu\text{rad}$  (FMHW) and (e) the energy resolution in eV.

## 2) The collimation-mode

In the collimation-mode the number of CRLs located in the optics hutch are chosen such that the beam divergence is minimized. The CRLs close to the sample position are not used. In this mode, the beam size is  $700 \times 300 \mu\text{m}^2$ , the divergence as low as  $0.5 \mu\text{rad}$  vertically. With the Si511 monochromator, the energy bandwidth is  $10^{-5}$  (see Fig. 7).

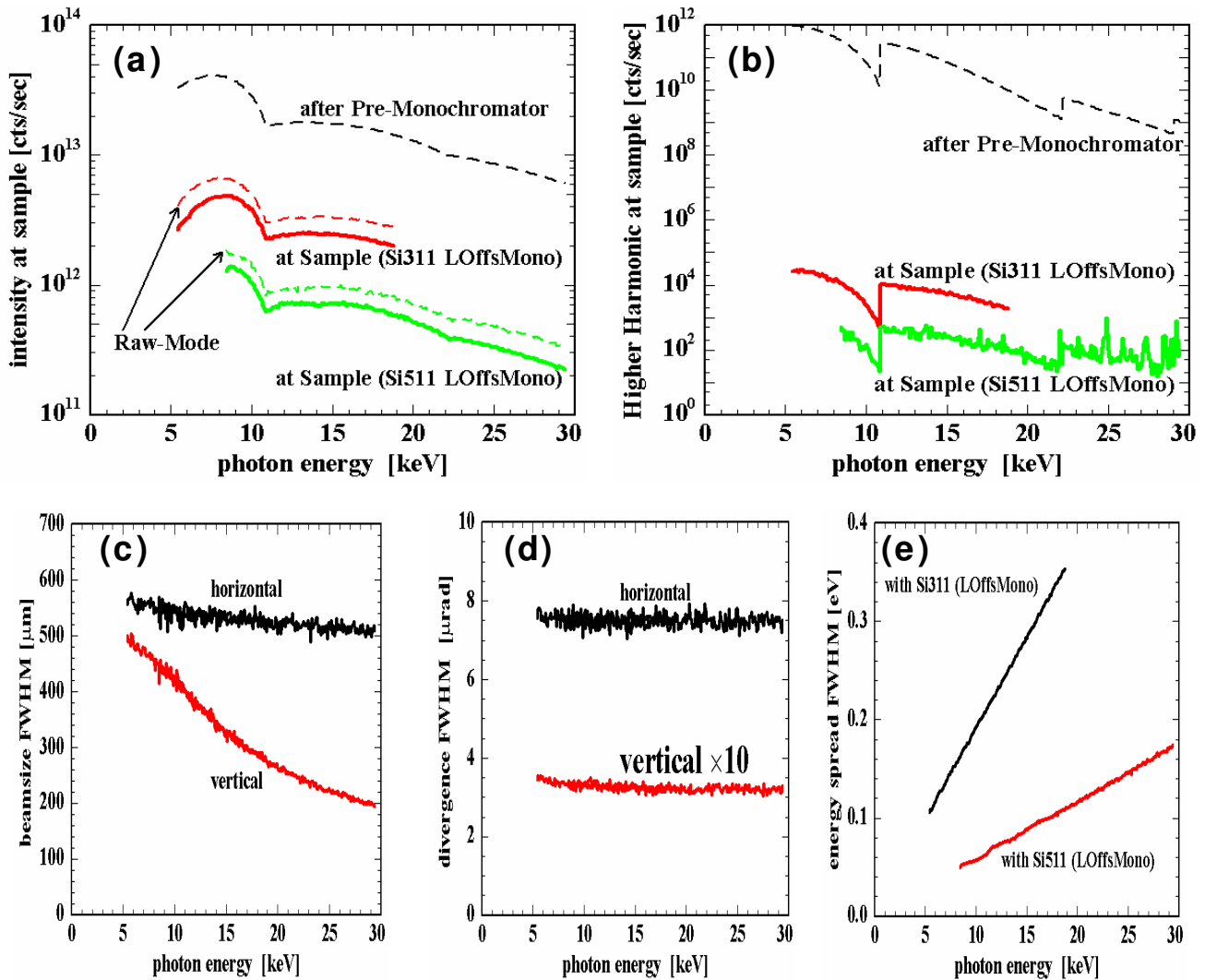


Figure 7: Parameters of the x-ray beam at the sample position using the collimation-mode at P08. Displayed are: (a) the intensity in counts per second, (b) the contamination due to higher harmonic photons in counts per seconds, (c) the beam size in  $\mu\text{m}$  (FWHM), (d) the divergence in  $\mu\text{rad}$  (FMHW) and (e) the energy resolution in eV.

### 3) The focusing-mode

In the focusing-mode the number of CRLs located in the optics hutch are chosen such that the beam size at the sample is minimized. The CRLs close to the sample position are not used. In the focusing-mode moderate focusing is realized with still very good resolving power in reciprocal space. In this mode, the beam size is  $200 \times 10 \mu\text{m}^2$ , the divergence is  $10 \mu\text{rad}$  vertically (see Fig. 8).

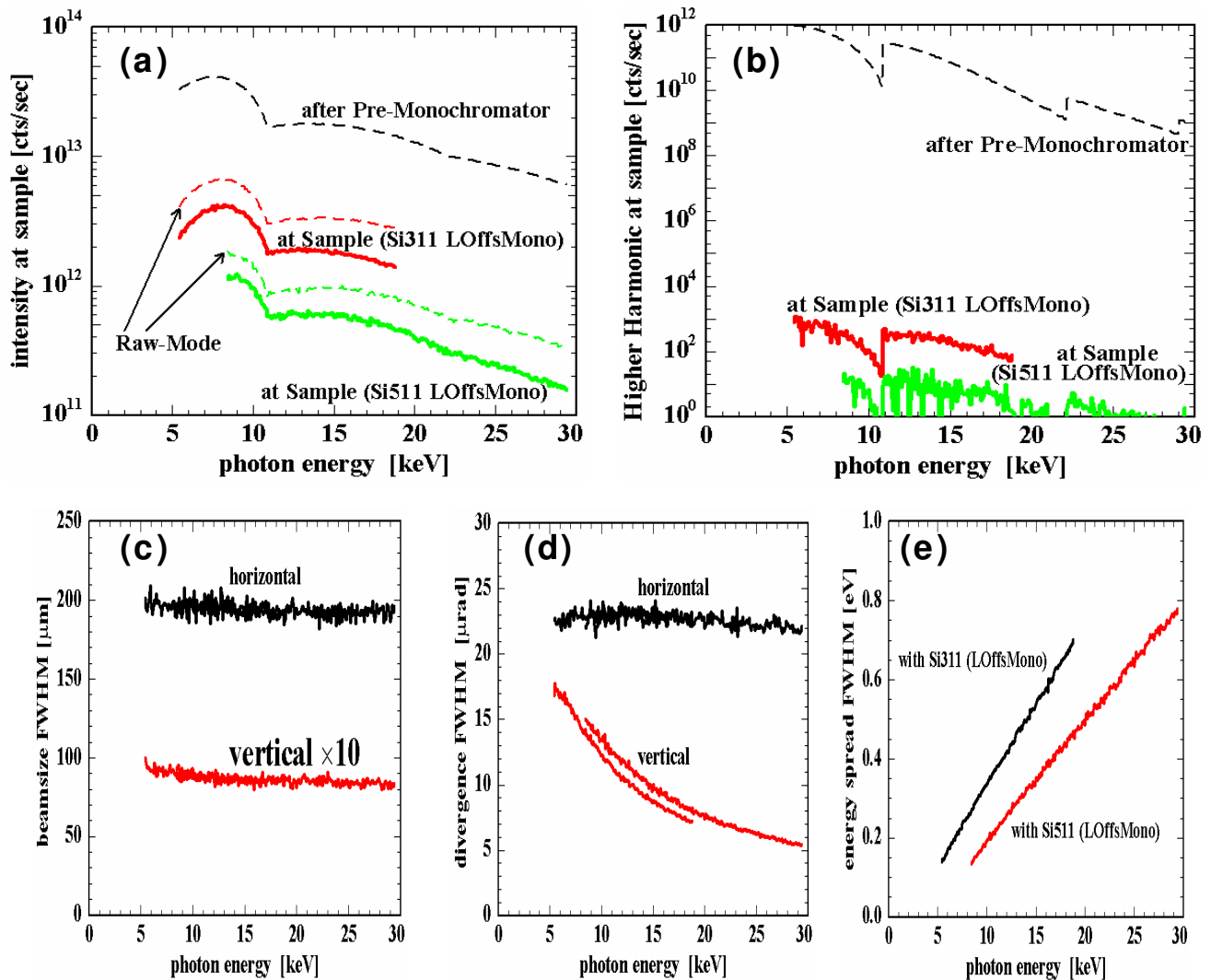


Figure 8: Parameters of the x-ray beam at the sample position using the focusing-mode at P08. Displayed are: (a) the intensity in counts per second, (b) the contamination due to higher harmonic photons in counts per seconds, (c) the beam size in  $\mu\text{m}$  (FWHM), (d) the divergence in  $\mu\text{rad}$  (FMHW) and (e) the energy resolution in eV.

#### 4) The $\mu$ -mode

In the  $\mu$ -mode the number of CRLs located in the optics hutch are chosen such that the divergence of the beam is minimized (collimation). The CRLs close to the sample are chosen such that the beam size at the sample is minimized. In this mode, the beam size is  $15 \times 2 \mu\text{m}^2$ , the divergence is  $120 \mu\text{rad}$  vertically with an energy bandwidth of  $10^{-5}$  (see Fig. 9).

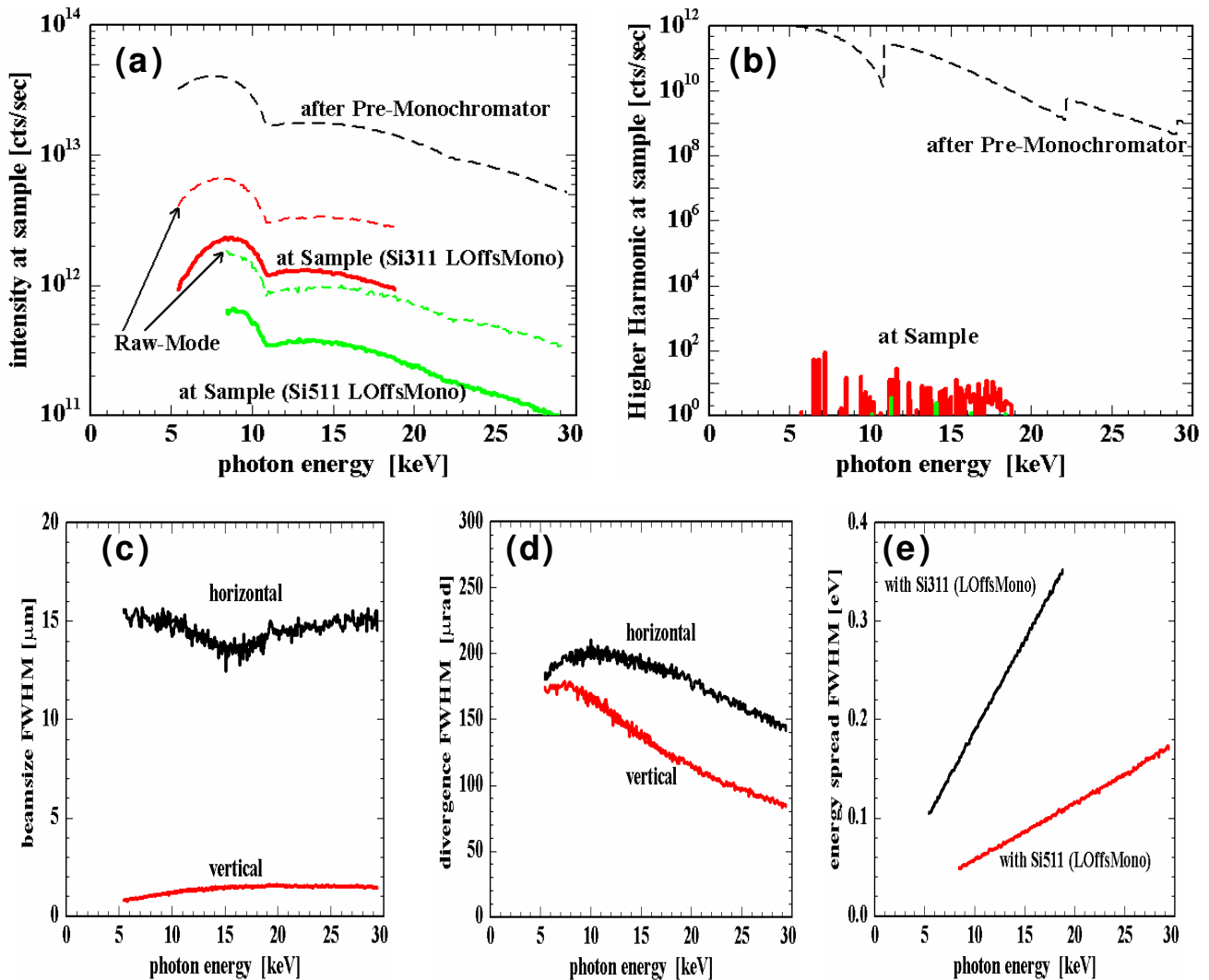


Figure 9: Parameters of the x-ray beam at the sample position using the  $\mu$ -mode at P08. Displayed are: (a) the intensity in counts per second, (b) the contamination due to higher harmonic photons in counts per seconds, (c) the beam size in  $\mu\text{m}$  (FWHM), (d) the divergence in  $\mu\text{rad}$  (FMHW) and (e) the energy resolution in eV.

## The experiment

A sketch of the experimental hutch of P08 is depicted in Fig 10. The x-ray beam enters the experimental hutch from the left and the beam is guided over an optical table with beam defining slits, absorbers and monitors. The beam is then led to the sample with a stability of better than  $5\mu\text{m}$  in position and better  $1\mu\text{rad}$  in direction. Samples can be mounted at the high precision six-circle diffractometer (Kohzu NZD-3) on the second optical table with 5 motorized degrees of freedom and 1t maximum load, or on the liquid diffractometer LISA. A sketch is shown in Fig. 10.

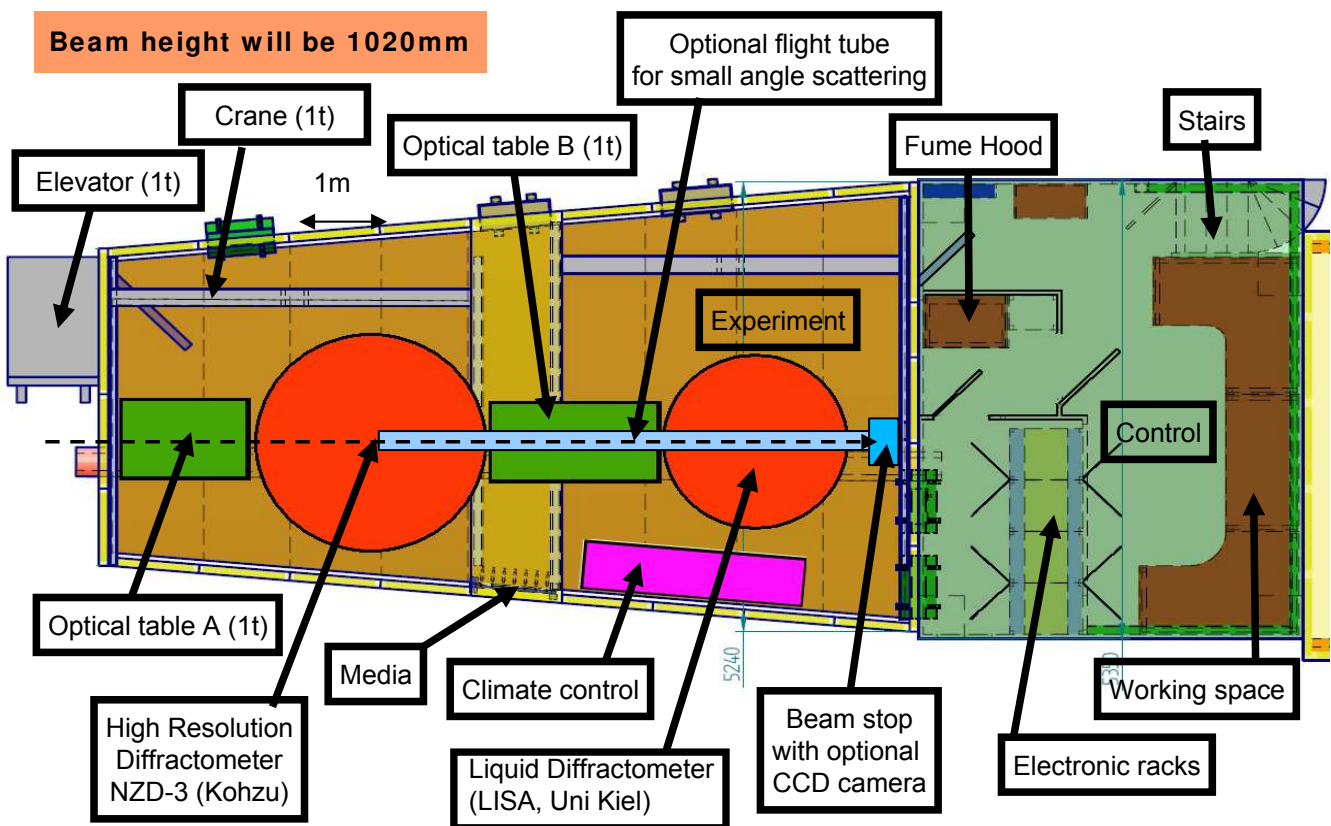


Figure 10: Sketch of the experimental hutch and the control hutch of P08.

P08 is equipped with several point detectors, a Mythen linear position sensitive detector, a Roper Scientific 4kx4k CCD ( $15\mu\text{m}$  pixel size) and an energy resolving VORTEX detector. The control hutch contains the electronics and a small chemical fume hood for cleaning samples at the beamline.

At the experimental hutch several media such as cooling water, and several gases are available. Small amounts of gases are also available at the fume hood in the control hutch.

## The optical tables A & B

Two optical tables (IDT) are installed in the experimental hutch, the first (Table A) 1.5m long, the second (Table B) 2m long. Both have 5 motorized degrees of freedom with high accuracy (see Fig. 11). The height of the table tops over the floor is 560mm at lowest position. This means 460mm distance to the x-ray beam (which is at 1020mm over the floor).

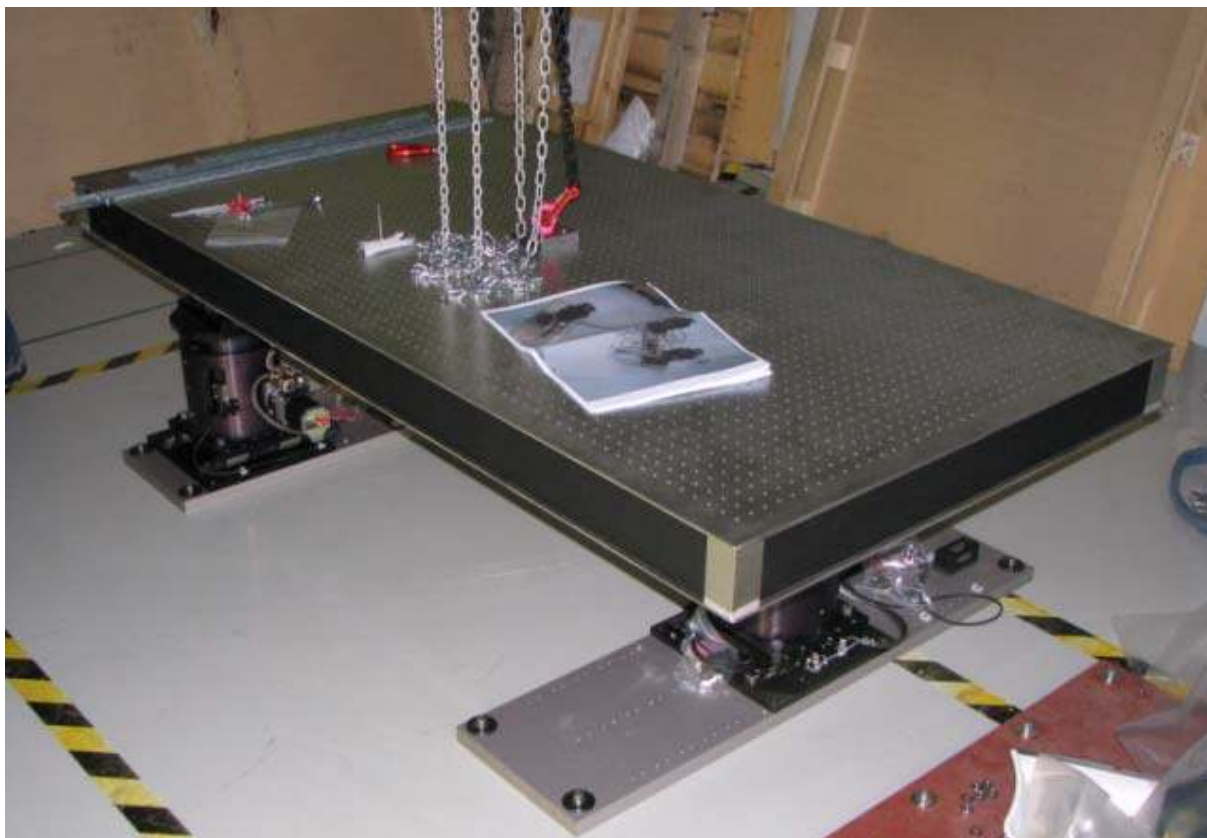


Figure 11: *The 2m long Table B*

The tables are equipped with 5 phase stepping motors and Renishaw encoders. The following specifications apply:

Translation vertical	= +/- 25mm	(resolution 0.2 $\mu$ m , repeatability 1 $\mu$ m)
Translation horizontal	= +/- 25mm	(resolution 1.5 $\mu$ m , repeatability 1 $\mu$ m)
Pitch	= +/- 1°	(resolution 0.1 $\mu$ rad, repeatability 1 $\mu$ rad)
Yaw	= +/- 1°	(resolution 3.0 $\mu$ rad, repeatability 1 $\mu$ rad)
Roll	= +/- 1°	(resolution 0.1 $\mu$ rad, repeatability 3 $\mu$ rad)

Each table can be loaded with 1t in the center.

The Table A usually carries the beam shaping optics (slits, monitors, absorbers). Table B usually carries the monochromator of the liquid diffractometer LISA.

### The 6-circle diffractometer NZD-3

The 6-circle diffractometer NZD-3 (Kohzu) is built for very high resolution applications. It is equipped with 5 phase stepping motors and with encoders on all main axes. Additional to the 6 rotations, 4 motors control the position and orientation of the whole diffractometer (table motors), 2 motors control the analyzer stage, 3 motors control xyz of the high precision sample stage and 3 motors control the heavy load cryostat sample stage (see Fig. 12).

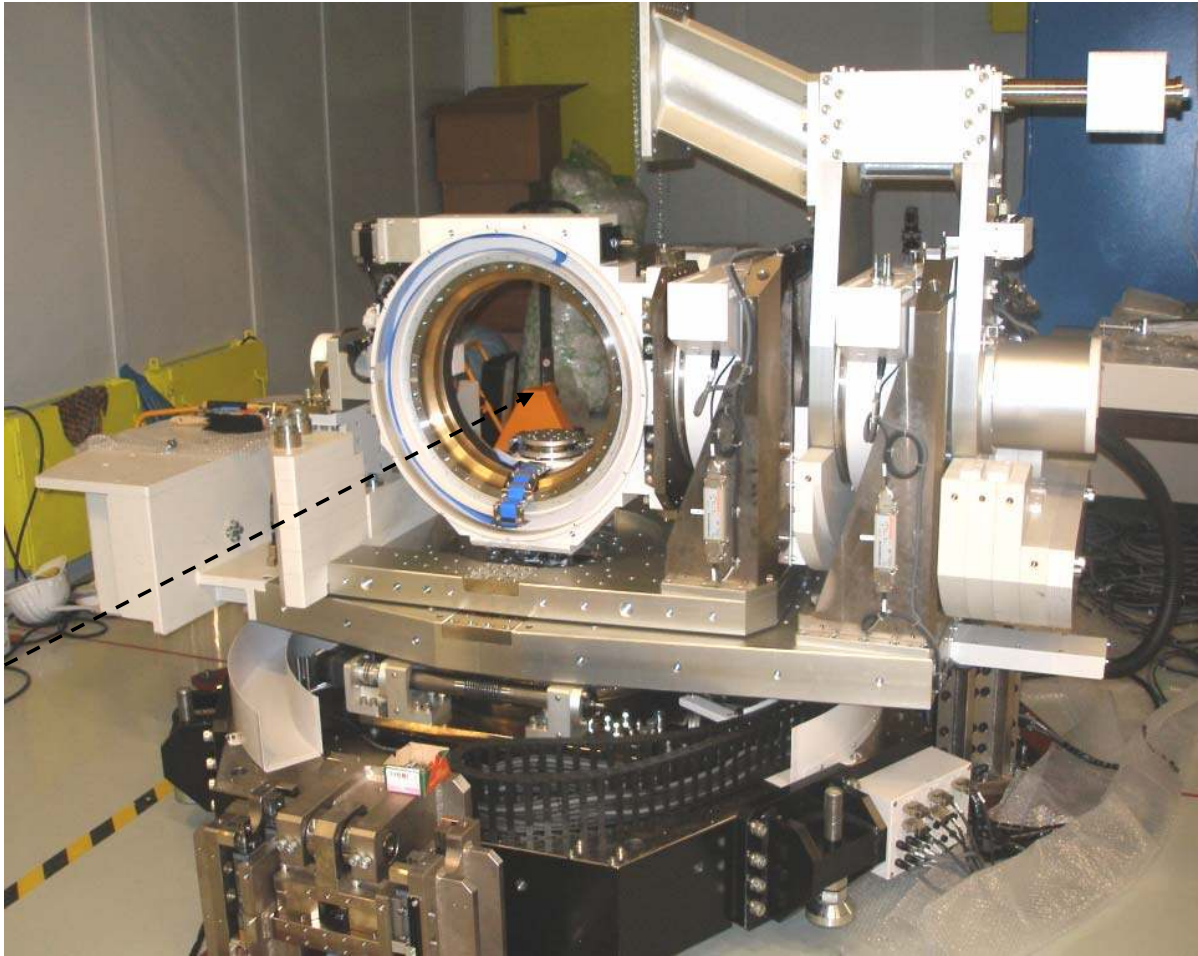


Figure 12: *The high precision 6-circle diffractometer NZD-3.  
The dashed line symbolizes the incident x-ray beam.*

The main rotations have a resolution of  $0.00005^\circ$  with a speed of  $4^\circ/\text{sec}$  and a full rotational repeatability of  $0.005^\circ$  even without encoder. The multiple motor sphere of confusion is less than  $20\mu\text{m}$  (see Fig 13).

The high precision sample stage can be loaded with 5kg and has a resolution of  $0.2\mu\text{m}$  in the movements of x, y and z. x and y have a travel-range of  $\pm 20\text{mm}$ , z of  $\pm 10\text{mm}$ . The heavy load sample stage can carry 20kg and has a resolution of  $0.2\mu\text{m}$  in the movements of x, y and z. x and y have a travel-range of  $\pm 2.5\text{mm}$ , z of  $\pm 5\text{mm}$ .

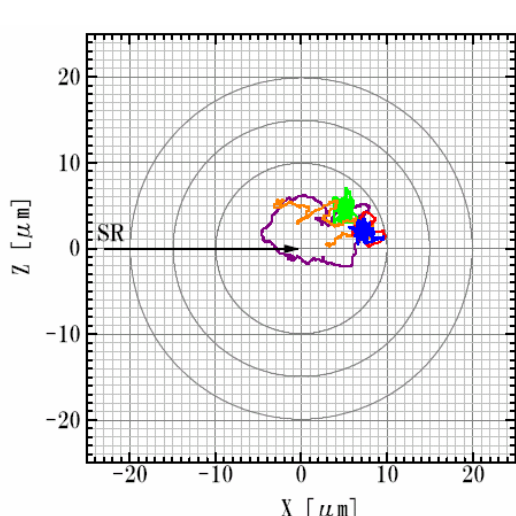


Fig. 12 SOC of OM, TT, CHELPHI s

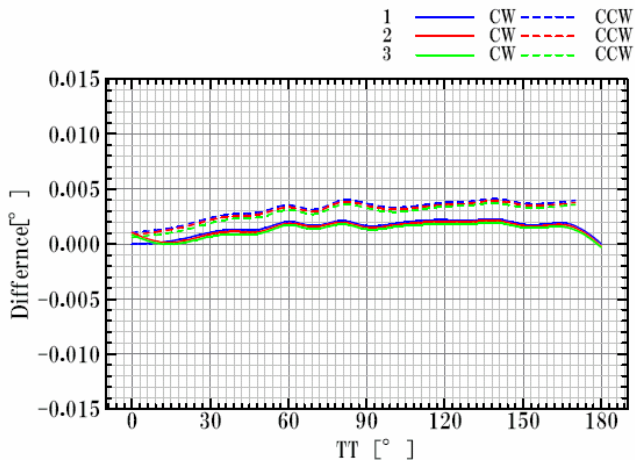


Fig. 9 Positional accuracy of OM and TT without feedback by encoder

Figure 13: *Left: sphere of confusion for motors Omega (incident angle), TwoTheta (detector angle) and Phi (sample azimuth) at different Chi (roll of the sample). Right: Repeatability of the motor TwoTheta*

### Ultra High Vacuum (UHV) Infrastructure at P08 (in planning phase)

The planned UHV-infrastructure is depicted in Figure 14. A UHV sputter and MBE-chamber in the P08 laboratory L045 which is close to the beamline will be installed. It should be equipped with Auger electron spectroscopy, LEED, MBE and Knudsen cell, a sputter gun and gas inlets. Microscopic methods such as AFM or SEM are also projected. The chamber is not designed yet and is scheduled for 2010.

At the beamline a UHV-Baby chamber with hemispherical Be-dome with 60mm diameter will be available. The chamber can be mounted to the MBE so that sample can be transferred in UHV. The baby chamber will utilize a heating up to  $T=1300K$  and a small ion getter pump which pumps the chamber to  $p < 10^{-9}mbar$ .

Furthermore, a UHV-catalysis/evaporation chamber will be available with a cylindrical Be windows with vertical sample surface orientation. This chamber will be used for in-situ measurements and is therefore equipped with a small MBE and Knudsen cells. It will be possible to attach it to the MBE-chamber in L047 and it can be transferred keeping the vacuum at  $p < 10^{-9}mbar$ . This chamber may also be used up to temperatures of  $T=1300K$ .

The baby chamber and the evaporation chamber will be available in 2010.



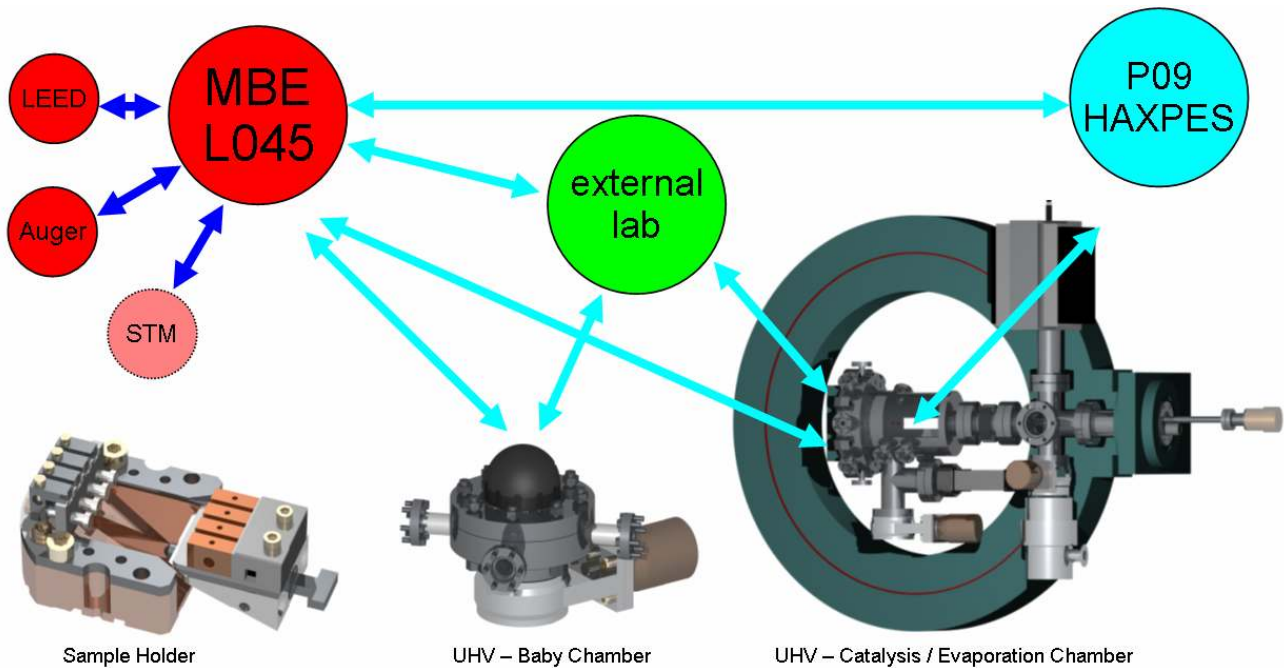


Figure 14: *Planned UHV-infrastructure at P08*

### The liquid diffractometer LISA

To investigate liquid surfaces and liquid-liquid interfaces the specially designed liquid diffractometer is required. This is based on the fact that for liquids the incident angle to the sample surface cannot be defined by rotating the sample. Instead, the x-ray beam has to be tilted by an additional monochromator. At standard liquid diffractometers this beam tilt is realized by simultaneously moving several motors including the sample height and position. This is a drawback at time critical measurements because a movement of the sample causes fluctuations on the liquid surface. As a consequence, University of Kiel (Germany) has designed a liquid interfaces scattering apparatus (LISA) and installed at P08. LISA completely avoids movements of the sample when the incident angle is changed. This is achieved by a double monochromator setup which can be rolled around the incident x-ray beam (see Fig. 15).

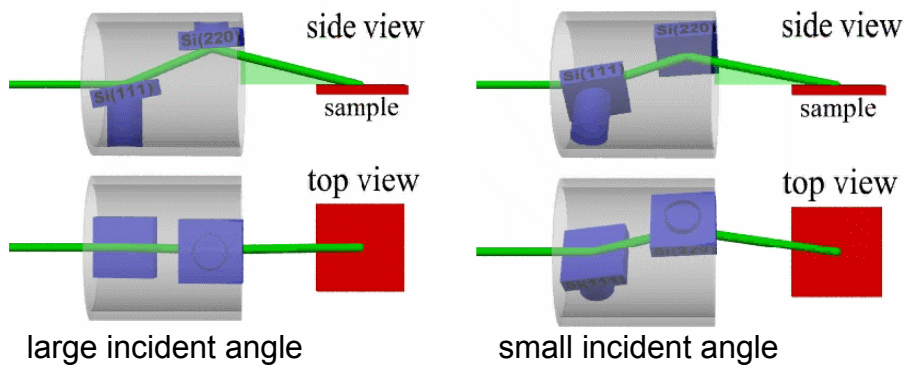


Figure 15: *LISA double monochromator rotated around the beam. Two incident angles are displayed*

LISA is fully tunable in photon energy from 6.4keV to 30keV. The accessible  $q$ -range of LISA is given by the double monochromator set. With the default Si111 and Si220 crystals the  $q$ -range is restricted to approximately  $2.6\text{\AA}^{-1}$ , depending on the photon energy (see Fig. 16). For most applications this value is sufficient.

At low photon energies and small incident angles the polarization effects at the LISA monochromator decrease the x-ray beam flux. In the worst case at 6.4keV the beam intensity is down by a factor of 10. At higher energy  $>15\text{keV}$  the effect becomes almost negligible (see Fig. 16). Figure 17 shows a sketch of LISA. LISA will be available in summer 2009.

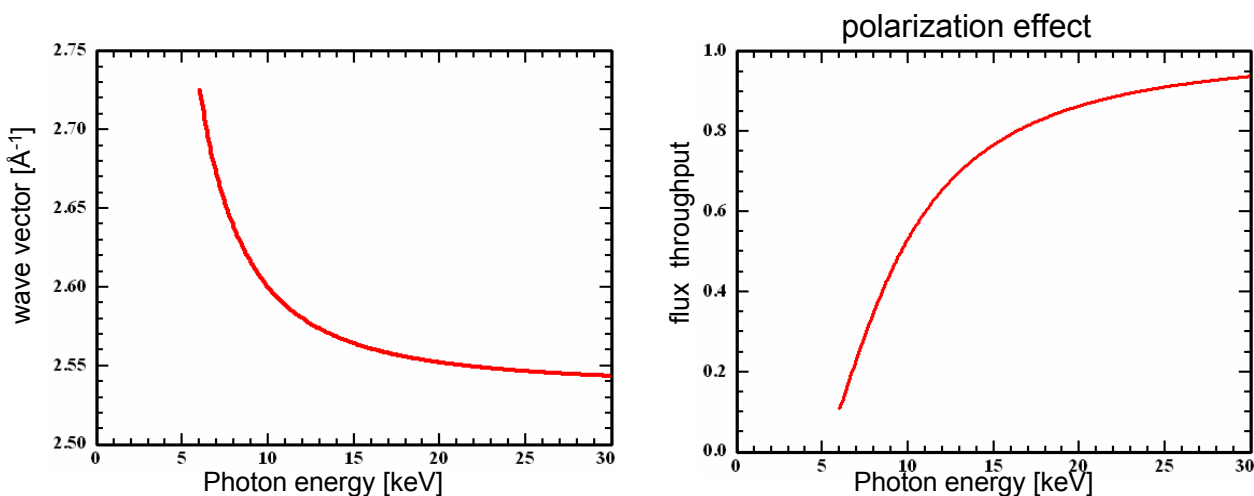


Figure 16: *Left: maximum wave vector transfer at LISA. Right: flux throughput through the LISA monochromator at incident angle 0 and depending on the photon energy.*

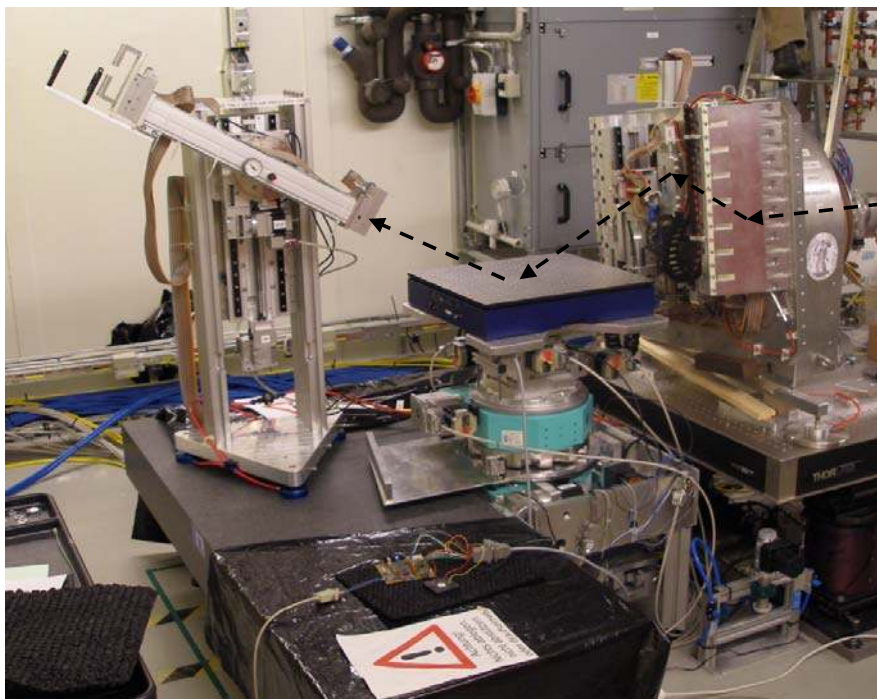


Figure 17: *Picture of LISA. The x-ray beam comes from the right (dashed line) and hits the double monochromator. The monochromator bends the beam down to the sample. The x-ray are then reflected to the detector on the left side.*